Laboratory Investigation (2019) 99:1906–1917
https://doi.org/10.1038/s41374-019-0310-1

ARTICLE

Antifibrotic effects of hypocalcemic vitamin D analogs in murine and human hepatic stellate cells and in the CCl_4 mouse model

Florian P. Reiter[1,2] · Liangtao Ye[1,2] · Florian Bösch[3] · Ralf Wimmer[1,2] · Renate Artmann[1,2] · Andreas Ziesch[1,2] · Veronika Kanitz[4] · Doris Mayr[4] · Christian J. Steib[1,2] · Michael Trauner[5] · Ivonne Regel[1,2] · Alexander L. Gerbes[1,2] · Julia Mayerle[1,2] · Simon Hohenester[1,2] · Enrico N. de Toni[1,2] · Gerald Denk[1,2]

Received: 18 December 2018 / Revised: 9 July 2019 / Accepted: 16 July 2019 / Published online: 29 August 2019

Abstract

Liver cirrhosis is a life-threatening consequence of liver fibrosis. The aim of this study was to investigate the antifibrotic potential of clinically available vitamin D analogs compared to that of calcitriol in vitro and in vivo. Murine hepatic stellate cells, Kupffer cells, and human LX-2 cells were treated with vitamin D analogs, and the profibrotic behavior of these cells was studied. In vivo liver fibrosis was induced using CCl_4 until measurable fibrosis was established. Animals were then treated with calcitriol and paricalcitol. Vitamin D and its analogs showed antifibrotic effects in vitro. Treatment with active vitamin D (calcitriol, CAL) and its analogs reduced the protein expression of α-smooth muscle actin (α-SMA) in mHSC. In human LX-2 cells alfacalcidol reduced transforming growth factor-β (TGF-β) induced platelet-derived growth factor receptor-β protein expression and contractility while paricalcitol (PCT), in its equipotent dose to CAL, reduced TGF-β induced α-SMA protein expression, and ACTA2 and TGF-β mRNA expression. No effects of a treatment with vitamin D and its analogs were observed in Kupffer cells. In vivo, PCT-treated mice had significantly lower calcium levels than CAL-treated mice. CAL and PCT reduced the hepatic infiltration of CD11b-positive cells and alanine transaminase levels, while PCT but not CAL significantly inhibited fibrosis progression, with a favorable side effect profile in the CCl_4 model. We conclude that hypocalcemic vitamin D analogs should be considered in future studies investigating vitamin D for the treatment of liver fibrosis.

Introduction

The progression of chronic liver disease to liver fibrosis and eventually cirrhosis often results in liver failure and hepatocellular carcinoma, and is a major cause of mortality and morbidity worldwide [1, 2]. Upon the initial episode of decompensation, the 5-year mortality rate without liver transplantation is 85% [1].

Although modern antiviral treatments are promising for decreasing hepatitis C virus (HCV)-related deaths in future years, many patients will still experience consequences of established liver cirrhosis. While the cessation of alcohol consumption is an effective therapy for many patients with alcoholic liver disease, other causes of chronic liver diseases, such primary sclerosing cholangitis, lack effective medical treatments.

In general the management of chronic liver diseases has improved. Here, a recent study by Caraceni et al. [3] demonstrated that overall survival can be prolonged in patients with decompensated cirrhosis by the long-term

Supplementary information The online version of this article (https://doi.org/10.1038/s41374-019-0310-1) contains supplementary material, which is available to authorized users.

✉ Florian P. Reiter
Florian.Reiter@med.uni-muenchen.de

1 Department of Medicine II, University Hospital, LMU, Munich, Germany

2 Liver Center Munich, University Hospital, LMU, Munich, Germany

3 Department of General, Visceral, and Transplantation Surgery, University Hospital, LMU, Munich, Germany

4 Institute of Pathology, University of Munich, Munich, Germany

5 Division of Gastroenterology and Hepatology, Department of Internal Medicine III, Medical University of Vienna, Vienna, Austria

administration of human albumin. This may result from an improvement of fluid balance [4] via an improvement of urinary sodium excretion [5] and amelioration of hyponatremia [6].

Despite these results that demonstrate an improvement in the management of chronic liver diseases, the development of effective antifibrotic therapies in chronic liver diseases remains an important unmet medical goal.

The development of liver cirrhosis results from progressive tissue damage. At the cellular level, liver fibrosis is mainly caused by hepatic stellate cells (HSCs), causing a progressive deposition of extracellular matrix proteins resulting in the loss of functional liver parenchyma [7] and the disruption of liver architecture, in turn determining portal hypertension [1]. Another important mechanism in the pathophysiology of liver fibrosis is the recruitment of inflammatory cells, which are responsible not only for cell damage but also for tissue repair and fibrosis development [8, 9].

The vitamin D receptor (VDR) is strongly expressed in nonparenchymal liver cells such as HSCs and Kupffer cells (KCs), but weakly expressed in hepatocytes [10]. In addition, the VDR is fully functional in HSCs and KCs [10]. The VDR was further identified as an important endocrine checkpoint of profibrotic behavior in HSCs, emphasizing the role of vitamin D (VD) in fibrogenesis in chronic liver diseases [11].

With an incidence rate higher than 90%, hypovitaminosis D is universal in patients suffering from chronic liver diseases [12]. The observations that a VD-deficient diet induces spontaneous liver fibrosis in mice [13], that 25-OH VD levels progressively decrease in more advanced stages of cirrhosis [14] and that low 25-OH VD serum levels are correlated with hepatic inflammation and fibrosis in patients with chronic hepatitis C [15] emphasize the importance of VD supplementation in chronic liver diseases.

Active VD metabolites such as 1,25 $(OH)_2$-vitamin D (calcitriol, CAL) and the VD analog calcipotriol (CPT) demonstrated encouraging effects on liver fibrosis in vitro and in vivo [11, 16, 17].

Despite widespread research activity about VD and its beneficial effects in liver diseases, a recent Cochrane analysis by Bjelakovic et al. [18] classified the overall quality of the evidence as very low. Therefore, further studies must address whether VD has relevant advantageous effects on chronic liver diseases.

The liver and kidney are the two organs that mediate hydroxylation at positions 1 and 25 in the VD activation process. Chronic liver insufficiency, which is frequently associated with kidney dysfunction, could be argued to interfere with the VD activation capacity in patients with liver diseases. The use of active metabolites or newer active VD analogs that have already demonstrated effects on liver fibrosis in preclinical settings, such as CAL [16, 17] or CPT [11], could remove this uncertainty. However, the use of CAL as a preventive long-term approach could result in harmful, potentially lethal complications such as hypercalcemia, nephrocalcinosis, or calciphylaxis.

Paricalcitol (PCT) is a hypocalcemic VD analog that demonstrated fewer calcemic side effects than CAL in the treatment of secondary hyperparathyroidism [19]. This advantage and the observation that, in contrast to CPT, PCT is available for systemic application (CPT is approved only for topical use in patients suffering from psoriasis) make PCT a therapeutic alternative to CAL and CPT.

The aim of this study was to investigate the effects of several VD analogs in comparison to those of CAL on profibrotic liver cell behavior. Furthermore, we investigated the effects of PCT, which appears to be the most viable active VD analog, in comparison to those of CAL in the CCl_4 mouse model.

Materials and methods

Murine hepatic stellate cells

Isolation of primary murine hepatic cells (mHSCs), reflecting hepatic mesenchymal cells, was performed by pronase-collagenase perfusion followed by density gradient centrifugation in 13.2% Nycodenz (Axis-Shield PoC, Norway) as described previously [20].

Murine hepatic kupffer cells

Isolation of primary murine hepatic Kupffer cells (mKCs) was performed by pronase perfusion followed by density gradient centrifugation in 17.5% Nycodenz (Axis-Shield PoC, Norway). mKCs were stimulated with 100 µg/l lipopolysaccharide (LPS) [21] for 24 h.

Cell culture

MHSC and LX-2 cells were maintained in Dulbecco's Modified Eagle Medium (Sigma-Aldrich, Germany) containing 10% (mHSC) or 2% (LX-2) fetal bovine serum (PAN-Biotech, Germany) and antibiotics (Sigma-Aldrich, Germany) in a humidified atmosphere with 5% CO2 and 21% O2 at 37 °C. Cells were treated with 1 µmol/l CAL (Cayman, USA), CPT (a kind gift from LEO Pharma, Denmark), alfacalcidol (ACD) (Cayman, USA), PCT (Cayman, USA), 4x PCT (4 µmol/l) (reflecting the equipotent CAL dose in vivo [19]) (Cayman, USA), doxercalciferol (DXC) (in different dosages up to 10 µmol/l) (Sigma-Aldrich, Germany), or 0.1% dimethyl sulfoxide (DMSO) (control) (Sigma-Aldrich, Germany). LX-2 cells were activated with 10 ng/ml transforming growth

factor-β (TGF-β) (Peprotech, Germany) and coincubated with VD analogs, as indicated.

LX-2 cells

LX-2 cells, as a liver derived mesenchymal human cell line, were purchased from Merck-Millipore (Germany). The authenticity of the LX-2 cells was analyzed by an external independent institution (Leibniz-Institut; DSMZ-Deutsche Sammlung von Mikroorganismen und Zellkulturen GmbH). LX-2 cells were classified as authentic according to the report of the external institution.

BrdU cell proliferation assay

The proliferation of LX-2 cells was measured using a BrdU assay kit (Roche, Germany) according to the manufacturer's instructions.

Water-soluble tetrazolium salt (WST) cell-viability assay

A WST assay was performed according to the manufacturer's instructions (Roche, Germany).

Immunofluorescence microscopy

MHSCs and LX-2 cells were fixed in 4% paraformaldehyde in phosphate-buffered saline (PBS) (Sigma-Aldrich, Germany), incubated with a monoclonal antibody against α-smooth muscle actin (α-SMA) (Sigma-Aldrich, Germany) in 5% bovine serum albumin (BSA) (Merck-Millipore, Germany), and detected with Alexa Fluor 488-labeled anti-mouse IgG (Molecular Probes, USA). MKCs were fixed in 4% paraformaldehyde in PBS (Sigma-Aldrich, Germany), incubated with a monoclonal antibody against CD163 (Santa Cruz Biotechnology, USA) in 5% BSA (Merck-Millipore, Germany) and detected with Alexa Fluor 488-labeled anti-mouse-IgG (Molecular Probes, USA). Nuclei were counterstained with Hoechst 33342 (Roche, Germany).

Real-time PCR

RNA was isolated using peqGOLD TriFast (Peqlab, Germany). Complementary DNA was synthesized accordingly. Real-time PCR was performed in a SYBR® Green system (QuantiTect SYBR Green PCR Kit, Qiagen, Netherlands) using a LightCycler 96® (Roche, Germany). Expression was calculated according to the ΔΔCt method with GAPDH and 36B4 as the housekeeping genes and normalized to the means of the controls. The primer sequences are shown in Table 1.

Migration assay

LX-2 cells were seeded in 12-well plates at 250,000 cells/well. After 24 h, a horizontal scratch was made in the confluent cells with a 100 µl pipette tip and washed with cell culture medium. Then, cells were stimulated under the

Table 1 Sequences of the PCR primers used

Genes	Fwd.	Rev.
Human		
GAPDH	5′-CAC CAG GGC TGC TTT TAA CT-3′	5′-TGA CGG TGC CAT GGA ATT TG-3′
36B4	5′-TGG GCA AGA ACACCA TGA TG-3′	5′-AAC ACA AAG CCC ACA TTC CC-3′
ACTA2	5′-TGC CCT GGT GTG TGA CAA TG-3′	5′-TCA CCC ACG TAG CTG TCT TT-3′
COL1α1	5′-ATG TGC CAC TCT GAC TGG AA-3′	5′-ACC AGT CTC CAT GTT GCA GA-3′
TGF-β	5′-TCA ACA CAT CAG AGC TCC GA-3′	5′-GTA TCG CCA GGA ATT GTT GCT-3′
PDGF-R	5′-AGG CAA GCT GGT CAA GAT CT-3′	5′-GCT GTT GAA GAT GCT CTC CG-3′
TIMP	5′-GTT TTG TGG CTC CCT GGA AC-3′	5′-GTC CGT CCA CAA GCA ATG AG-3′
MMP2	5′-AGA AGT ATG GCT TCT GCC CT-3′	5′-CTT GCG GTC ATC ATC GTA GTT-3′
MMP9	5′-CTT TGA GTC CGG TGG ACG AT-3′	5′-TCG CCA GTA CTT CCC ATC CT-3′
Murine		
Gapdh	5′-AGT ATG ACT CCA CTC ACG GC-3′	5′-ATG TTA GTG GGG TCT CGC TC-3′
36B4	5′-TCT AGG ACC CGA GAA GAC CT-3′	5′-CCC ACC TTG TCT CCA GTC TT-3′
Tgf-β	5′-CGC AAC AAC GCC ATC TAT GA-3′	5′-ACT GCT TCC CGA ATG TCT GA-3′
Mcp	5′-GCT GCT ACT CAT TCA CCA GC-3′	5′-CTT CTT GGG GTC AGC ACA GA-3′
TnfNF-α	5′-CAG AAA GCA TGA TCC GCG AC-3′	5′-TAG ACA GAA GAG CGT GGT GG-3′
Il-18	5′-ACA ACT TTG GCC GAC TTC AC-3′	5′-GTC TGG TCT GGG GTT CAC TG-3′
Il-6	5′-TAC CAC TCC CAA CAG ACC TG-3′	5′-CAA GTG CAT CAT CGT TGT TCA-3′
Il-1β	5′-ACT CAT TGT GGC TGT GGA GA-3′	5′- CAT GAG TCA CAG AGG ATG GG-3′

The sequences of all primers used in this study are listed in the table

indicated test conditions for an additional 24 h. Images at x5 magnification were acquired before and after incubation with the test substances. The cell-free area was measured with ImageJ software (USA). The reduction in the initial area was calculated.

Collagen gel contraction assay

LX-2 cells were plated at a density of 200,000 cells per well in 12-well plates. The gel contraction assay was performed as described by Bell et al. [22]. Briefly, cells were seeded in 1% collagen (Corning, USA). Thirty minutes after polymerization of the collagen, the gel was mobilized from the surface using a pipette tip. Medium containing stimulating agents was added to the gels. After 24 h of incubation, the gel area was measured using ImageJ software (USA). The ratio of the well area to the gel area was calculated.

Immunoblotting

Cells were lysed in a standard protein lysis buffer. Protein concentrations were measured with Bradford reagent (Bio-Rad, Germany). Protein was loaded in equal amounts and separated by sodium dodecyl sulfate polyacrylamide gel electrophoresis, followed by transfer to polyvinylidene difluoride membranes (Merck-Millipore, Germany). Membranes were incubated with monoclonal antibodies against α-SMA (Sigma-Aldrich, Germany), platelet-derived growth factor receptor-β (PDGF-R) (Cell Signaling Technology, USA), and GAPDH (Abcam, UK). This incubation was followed by incubation with a goat anti-mouse IgG-HRP (Bio-Rad, Germany), goat anti-rabbit IgG-HRP (Bio-Rad, Germany), or goat anti-sheep IgG-HRP (R&D Systems, USA) antibody. Visualization was performed using a ChemoCam (INTAS, Germany) after incubation with Clarity™ Western ECL Substrate (Bio-Rad, Germany).

Animal experiments

Liver fibrosis was induced using CCl_4 (Sigma-Aldrich, Germany) dissolved in corn oil (Sigma-Aldrich, Germany). Male C57BL/6 mice were purchased from Charles River (Germany) and were challenged three times weekly with intraperitoneal (i.p.) injections of CCl_4 (the first dosage was 0.25 ml/kg body weight (b.w.), followed by 0.5 ml/kg b.w.) beginning at 8 weeks of age for 3 months (Fig. 1). After 4 weeks of CCl_4 treatment, which was intended to induce clinically measurable liver fibrosis at the point of therapeutic intervention, treatment with CAL and equipotent PCT [19] was started in parallel to the CCl_4 injections for 8 weeks (Fig. 1). CAL diluted in DMSO was administered in five i.p. doses at a cumulative weekly dosage of 1 µg/100 g b.w. The weekly dosage of CAL was chosen according to a previous work by Abramovitch et al. [17], which demonstrated the antifibrotic potency of the described dosage against thioacetamide-induced liver fibrosis in rodents. PCT diluted in DMSO was administered in 5 weekly i.p. doses at a cumulative weekly dosage equipotent to that of CAL of 4 µg/100 g b.w. [19]. Control animals and CCl_4 mice received vehicle (corn oil or DMSO). The animals were housed on a 12/12 h light/dark cycle and were fed ad libitum. Animals were maintained according to local regulations. All animals received humane care, and the study protocols complied with the institution's guidelines. All institutional and national guidelines for the care and use of laboratory animals were followed. The experiments were approved by the local authorities (Regierung von Oberbayern).

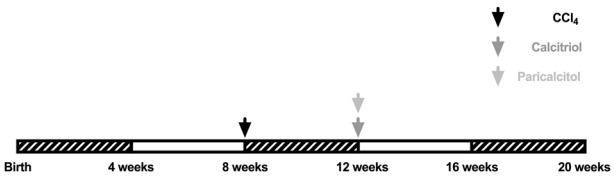

Fig. 1 Study design in vivo. Liver fibrosis was induced using CCl_4 in mice at 8 weeks of age. After 4 weeks of CCl_4 administration, animals histologically showed F2 to F3 fibrosis (see also Fig. 6), and treatment with CAL and equipotent PCT was initiated in parallel with CCl_4 injection. Animals were sacrificed at 20 weeks of age

Sirius red staining

Liver samples were fixed using 4% formaldehyde. After embedding in paraffin, 4-µm sections were stained with Sirius red according to standard protocols. Slides were scanned using a Pannoramic MIDI II® digital slide scanner from 3D-Histech (Sysmex, Norderstedt, Germany). The stained fibrotic area on the Sirius red-stained slides was quantified via QuPath software (UK) and ImageJ software (USA).

Metavir and desmet scoring

Histological scoring according to the Metavir [23] and Desmet [24] scoring systems was performed by two pathologists (VK and DM).

Immunohistochemistry

Paraffin-embedded sections (3 µm) of liver tissues were used for CD11b immunohistochemical staining. An anti-CD11b monoclonal rabbit antibody (Abcam, UK) was applied as the primary antibody and detected by an EnVision + System HRP-labeled polymer anti-rabbit antibody (Dako, USA). CD11b-positive cells were quantified in ten

fields of view per mouse at a magnification of x10 by ImageJ software (USA).

Serum biochemistry

Bilirubin, alanine transaminase (ALT), alkaline phosphatase (AP), urea, and calcium were analyzed using a respons® 910 analyzer (Diasys, Germany).

Statistical analysis

Statistical calculations were performed with the SPSS 25 software package (IBM, USA) using a two-tailed Student´s *t*-test, a chi-squared test or analysis of variance (ANOVA), as applicable. When a relevant influence was observed in an experiment, univariate ANOVA was performed, and the degrees of freedom, means of squares and *F*-values were calculated. The model of total variance reflects the variance in cell preparation, treatment, and residual error. p-values <0.05 were considered statistically significant. Data are presented as the means ± standard errors of the mean.

Results

VD analogs inhibit the spontaneous activation of murine HSCs and counteract the TGF-β-mediated profibrotic behavior and contractility of human LX-2 cells

We previously reported the inhibitory effects of CAL on primary murine HSC activation and profibrotic behavior [16]. Here, we conducted experiments to compare the efficacy of CAL and different VD analogs on the spontaneous activation of HSCs.

All VD analogs used significantly reduced α-SMA protein expression, a marker of activation and a hallmark of liver fibrosis, in murine HSCs compared to that in control cells (Figs. 2a and 3). These effects are shown in representative western blots and immunofluorescence staining for α-SMA (Fig. 2b, c).

We next investigated the antifibrotic effects of different VD analogs on TGF-β-mediated profibrotic HSC behavior in human LX-2 cells. Here, we observed a reducing trend under stimulation with CAL and VD analogs, while a significant reduction in α-SMA protein expression compared to that induced by TGF-β was observed only for the dose of PCT that was equipotent to CAL in vivo (4x PCT) (Fig. 4a). Furthermore, the expression of PDGF-R, another marker of HSC activation, was significantly reduced in LX-2 cells stimulated with the VD analog ACD compared to its change in response to TGF-β (Fig. 4b). However, the other VD analogs tested only showed a reducing trend (Fig. 4b and Supplementary Fig. 3). The representative immunofluorescence staining results illustrate these effects on α-SMA protein expression (Fig. 4c). In addition to their characteristic expression of α-SMA, activated HSCs generally demonstrate typical properties of increased proliferation, high-migration potential and contractile behavior. Thus, we assessed these cellular features under treatment with VD analogs with various assays.

Here, we observed a significantly lower reduction in the initial gel area under stimulation with ACD compared to that seen with TGF-β stimulation, demonstrating the anticontractile effects of the VD analog ACD (Fig. 4d, e). Although the differences were not statistically significant, the other VD analogs showed a tendency to reduce contractile forces similar to that shown by ACD (Fig. 4d, e). In the BrdU assay, no differences in cell proliferation were found under stimulation with CAL or the VD analogs in LX-2 cells (Supplementary Fig. 1A). Upon treatment of LX-2 cells with CAL, ACD, PCT, and 4x PCT, we observed a nonsignificant reduction in the cell migration potential (Supplementary Fig. 1B), possibly indicating an inhibition of migration, as cell proliferation did not differ as measured by the BrdU assay. We further observed by real-time PCR that 4x PCT reduced TGF-β-induced ACTA2 and TGF-β messenger RNA (mRNA) expression (Fig. 5a, b). Interestingly, we observed a reduction in matrix metalloproteinase-2 (MMP2) expression under VD treatment compared to that seen under TGF-β treatment (Supplementary Fig. 1C). No treatment-associated differences in mRNA expression were observed for PDGF-R, collagen 1α1 (Col1α1), MMP9, and tissue inhibitor of metalloproteinase (TIMP) (Supplementary Fig. 1D–G). Incubation of LX-2 cells with doxercalciferol (DXC) in increasing doses (up to 10 µmol/l) did not result in a significant reduction of TGF-β-mediated α-SMA protein expression. Nevertheless at 10 µmol/l DXC there was a tendency towards reduced α-SMA expression (Supplementary Fig. 3). However, this was accompanied by a decrease (not significant) in metabolic activity as measured by the WST assay. This may indicate beginning cytotoxicity at these high doses (Supplementary Fig. 2B) in contrast to a normal cell viability in the other vitamin D analogs (Supplementary Fig. 2A).

In summary, VD analogs demonstrated efficacy in inhibiting profibrotic HSC behavior in vitro in murine HSC and less definite in human LX-2 cells.

Expression of fibrogenic and inflammatory genes in mKCs treated with VD and its analogs

KCs are major players in the development of liver fibrosis and are one of the main sources of TGF-β production, which leads to the transdifferentiation of quiescent HSCs to activated

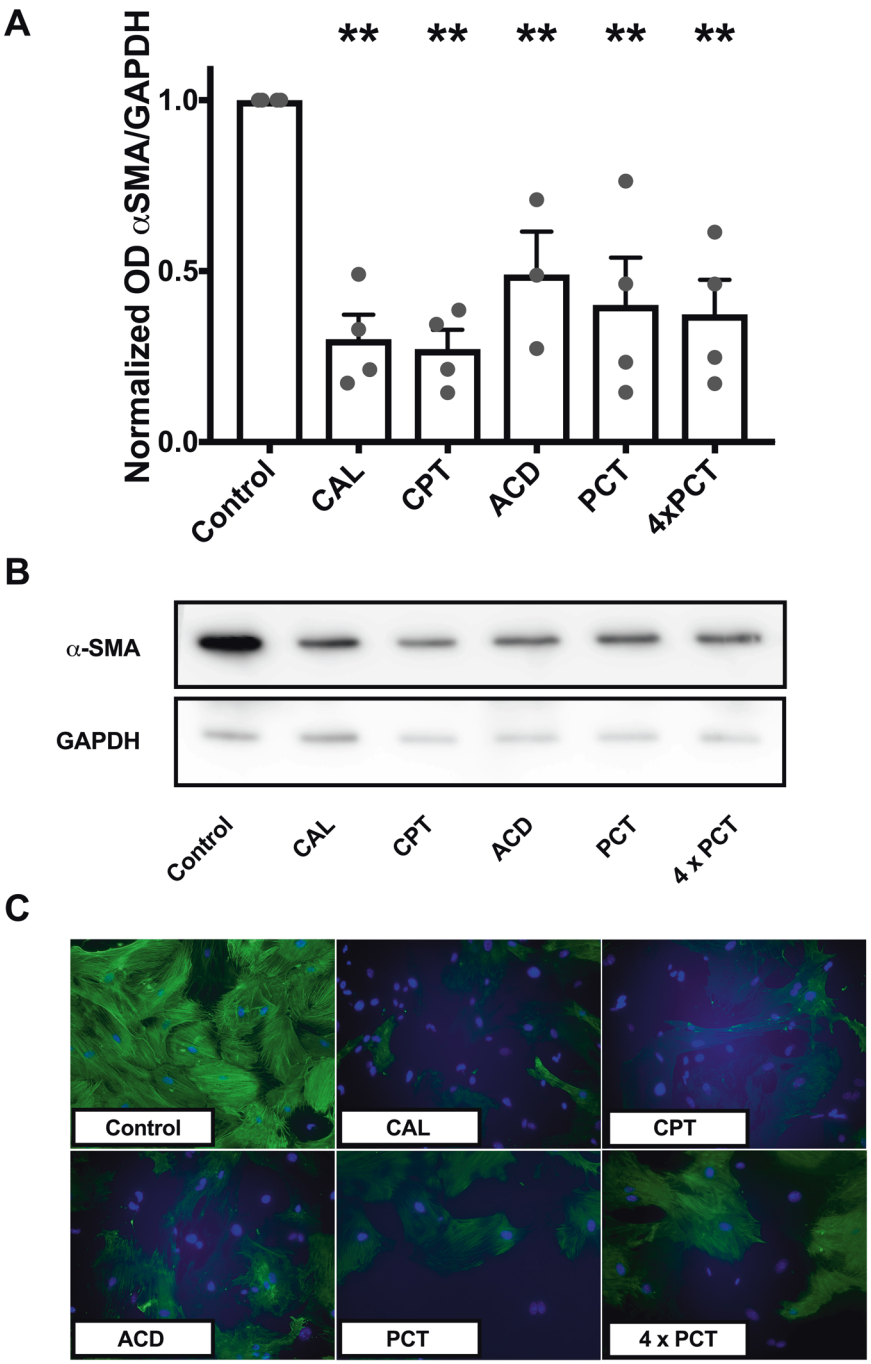

Fig. 2 Vitamin D and its analogs inhibit the spontaneous activation of murine hepatic stellate cells. Murine hepatic stellate cells (mHSCs) were plated on uncovered plastic for 14 days, and their spontaneous activation behavior under treatment with calcitriol (CAL) and clinically available vitamin D analogs (calcipotriol, CPT; alfacalcidol, ACD; paricalcitol, PCT) was studied. **a** The protein expression of α-smooth muscle actin (α-SMA) normalized to that of GAPDH was quantified by densitometry. The values shown are normalized to the control group ($n = 3$–4, $^{**}p < 0.01$; ANOVA). **b** Representative blots are shown. **c** Murine HSCs were labeled with α-SMA (green). Nuclei (blue) were stained with Hoechst 33342. Treatments decreased α-SMA expression in mHSCs, as shown

myofibroblasts [9, 25]. Furthermore, LPS was demonstrated to stimulate KCs with respect to inflammation and profibrotic signaling [26]. We therefore studied the effects of VD and its analogs on the mRNA expression of fibrosis-related genes in mKCs with and without LPS challenge.

Isolated cells were stained for the macrophage marker CD163 and exhibited positive signals (Supplementary Fig. 4A). We did not observe significant effects of VD or its analogs on the expression of the tested genes (Tgf-β, tumor necrosis factor-α (Tnf-α), monocyte chemotactic protein-1 (Mcp), interleukin (Il) 18, Il-6, and Il-1β) with or without LPS stimulation (Supplementary Fig. 4B–G). In summary, we could not identify beneficial effects of VD and its analogs on the proinflammatory and profibrotic behavior of mKCs as tissue-specific macrophages and profibrotic mediators in the liver.

The CCl_4 protocol used induces clinically detectible fibrosis after 4 weeks of treatment

In this study, we intended to simulate a clinical setting in which VD treatment starts as a consequence of detected

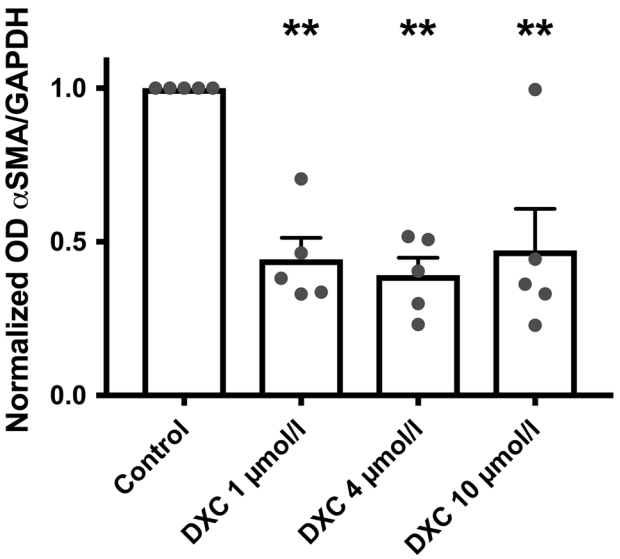

Fig. 3 Doxercalciferol reduces α-SMA expression in murine hepatic stellate cells. Murine hepatic stellate cells were plated on uncovered plastic for 14 days. Their spontaneous activation behavior under treatment with different dosages of doxercalciferol (DXC), a clinically available vitamin D analog, was assessed, and the protein expression of α-smooth muscle actin (α-SMA) normalized to that of GAPDH was quantified with densitometry. The values shown are normalized to the control group ($n = 5$, $^{**}p < 0.01$; ANOVA)

liver fibrosis. We therefore induced liver fibrosis using CCl_4 for 4 weeks. After 4 weeks, we observed pronounced liver fibrosis (stage F2 to F3) as assessed by Metavir and Desmet, two scoring systems used in clinical practice, in CCl_4-treated animals (Fig. 6a, b). The measured extent of liver fibrosis is shown in the representative images of Sirius red staining (Fig. 6c). As expected, after 4 weeks of treatment, significantly higher values of ALT were observed in animals treated with CCl_4 than in control animals (Supplementary Fig. 5). Interestingly, the spleen/body ratio was significantly lower in CCl_4-treated animals than in control animals at this time point (Supplementary Fig. 5). However, the body weight, liver/body weight ratio, and AP values did not differ significantly (Supplementary Fig. 5).

These results confirm that compared to control animals, CCl_4-treated animals exhibit F2 to F3 fibrosis at the point of intervention and show clinically detectable fibrosis. This situation is the experimental in vivo counterpart of the clinical situation when an antifibrotic intervention should be started.

CAL and PCT show beneficial effects on inflammatory liver damage in CCl_4-challenged mice, while PCT also demonstrates a favorable side effect profile compared to CAL

As a next step, we sought (i) to clarify whether the hypocalcemic VD analog PCT is as potent as CAL in conferring hepatoprotection in the CCl_4 model and (ii) to perform a head-to-head comparison of the side effect profiles of both agents.

Over time, corn oil-treated control animals gained more weight than CCl_4-treated animals (Fig. 7a). Although $CCl_4 + PCT$ group animals had no profound weight loss over time (Fig. 7a), $CCl_4 + CAL$-treated animals had significantly lower body weights than animals in all the other groups (Fig. 7a). We initially planned to challenge the animals with CCl_4 for 16 weeks instead of 12 weeks, but due to the pronounced weight loss in the $CCl_4 + CAL$ group, we terminated this experiment at an earlier time point. The final weights at the time of experiment termination show the lower weights of animals in the $CCl_4 +$ CAL group than animals in the other groups (Fig. 7b). The livers of animals in the $CCl_4 + CAL$ group weighed significantly less when normalized to the body weight than those in the other CCl_4-treated groups (Fig. 7c). The spleen/body weight ratio was significantly higher in CCl_4-treated animals than in animals in the other groups, possibly indicating portal hypertension (Fig. 7d). Notably, the CCl_4–group had a higher ALT level than the other groups, indicating the beneficial effects of CAL and PCT (Fig. 7e). Analysis of bilirubin levels showed that the highest increase occurred in the $CCl_4 + CAL$ group, while the $CCl_4 + PCT$ group exhibited lower bilirubin levels than the $CCl_4 + CAL$ group that were statistically different from those in the CCl_4 group (Fig. 7f). In addition, the serum urea levels were significantly lower in the $CCl_4 + CAL$ and $CCl_4 + PCT$ groups than in the CCl_4 group (Fig. 7g), indicating that renal function was not impaired under CAL or PCT therapy. Finally, PCT was less calcemic than CAL (Fig. 7h).

Taken together, these results indicate that the side effect profile of PCT is superior to that of CAL. Furthermore, PCT showed anti-inflammatory effects comparable to those of CAL, without such weight loss and hyperbilirubinemia.

PCT but not CAL significantly inhibits the progression of liver fibrosis in the CCl_4-model, while both CAL and PCT reduce the infiltration of CD11b-positive cells into the liver

To quantify the fibrotic area in liver slides stained with Sirius red, we used an image analysis system. We observed a reduction in the fibrotic area under PCT treatment (Fig. 8a, b), in addition to a reduction in the spleen/body weight ratio as an indirect marker of fibrosis and portal hypertension. These findings are shown in representative images of liver slides stained with Sirus red indicating a reduction in fibrosis in the treatment group. We further assessed the infiltration of CD11b-positive cells into the liver and found significant infiltration in CCl_4-treated animals compared to that in control animals (Fig. 8c–e), indicating that inflammation was increased in CCl_4-treated animals. Interestingly, both CAL

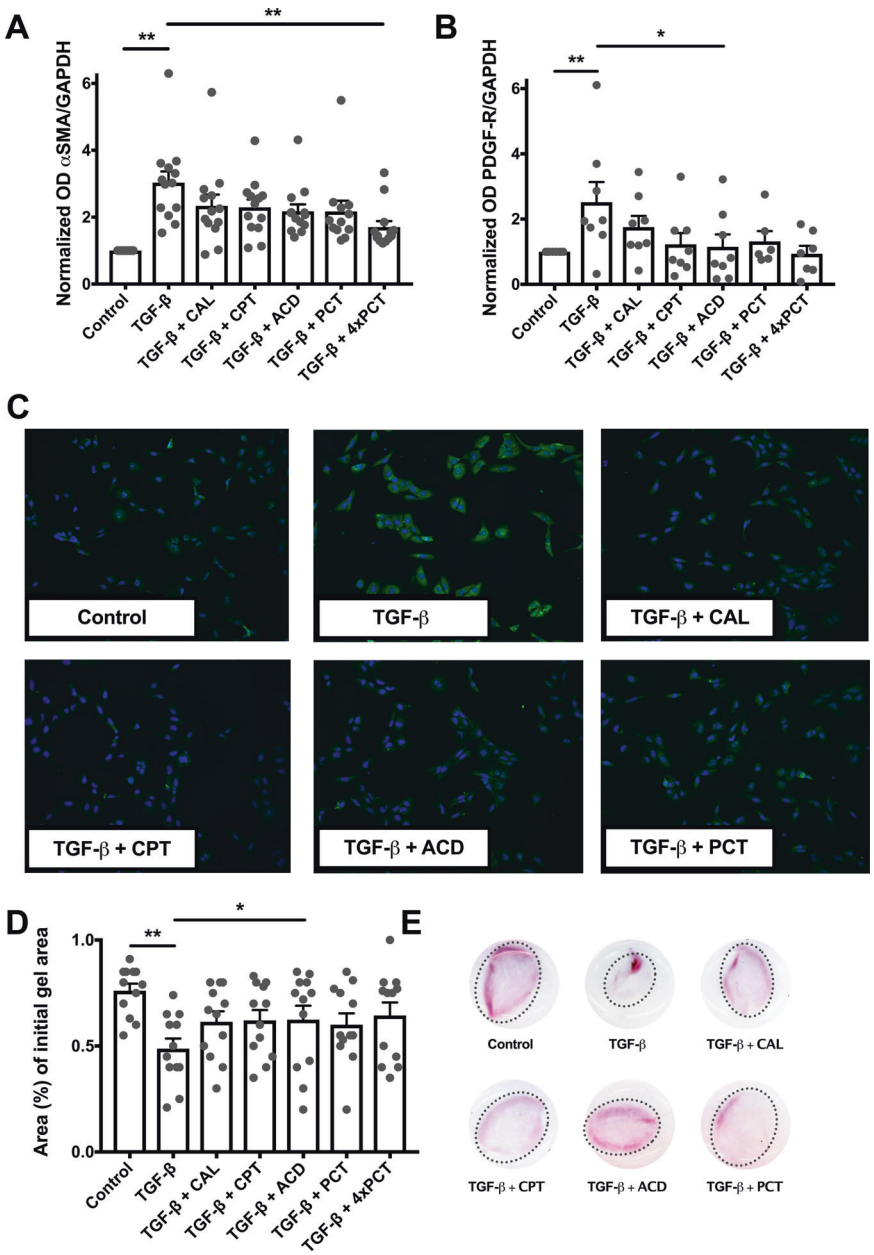

Fig. 4 Effects of vitamin D and its analogs on TGF-β-mediated profibrotic behavior in human LX-2 cells. Human LX-2 cells were activated using transforming growth factor-β (TGF-β). Profibrotic behavior under TGF-β stimulation and treatment with calcitriol (CAL) and clinically available vitamin D analogs was studied (calcipotriol, CPT; alfacalcidol, ACD; paricalcitol, PCT). **a**, **b** Protein expression of α-smooth muscle actin (α-SMA) and platelet-derived growth factor receptor-β (PDGF-R) normalized to GAPDH expression was quantified by densitometry. The values were normalized to the control group ($n = 6$–13; $^{*}p < 0.05$; $^{**}p < 0.01$; ANOVA). **c** LX-2 cells were labeled with a-SMA (green). Nuclei (blue) were stained with Hoechst 33342. Treatment of LX-2 cells diminished TGF-β-mediated α-SMA expression, as illustrated. **d**, **e** A collagen gel contraction assay was performed to study the inhibitory effects of vitamin D and its analogs on TGF-β-mediated contractility in human LX-2 cells. The gel area as a percent of the initial gel area ($n = 11$–12, $^{*}p < 0.05$; $^{**}p < 0.01$; ANOVA) and representative images after stimulation are shown

and PCT significantly reduced the infiltration of CD11b-positive cells under CCl_4 challenge, indicating the anti-inflammatory effects of both agents (Fig. 8c–e).

Taken together, these results demonstrate significant prevention of hepatic inflammation under treatment with both CAL and PCT, while fibrosis progression was prevented under treatment with PCT but not with CAL.

Discussion

In this study, we demonstrated that clinically available VD analogs have antifibrotic potency in mHSCs and LX-2 cells in vitro. We showed that in LX-2 cells PCT reduced α-SMA protein expression and ACTA2 and TGF-β mRNA expression, a finding that might indicate the superiority of this VD analog to CAL, which did not significantly affect these markers of fibrosis. We further showed that ACD exhibited anticontractile effects in the gel contraction assay, while only a trend was seen with the other VD analogs. This observation could explain the findings of our in vivo experiments in animals treated with CAL and PCT, which exhibited a decreased spleen/body weight ratio as an indirect marker of portal hypertension. This finding is in accordance with that of a study by Lee et al. [27], who described a comparable magnitude of reduction in portal

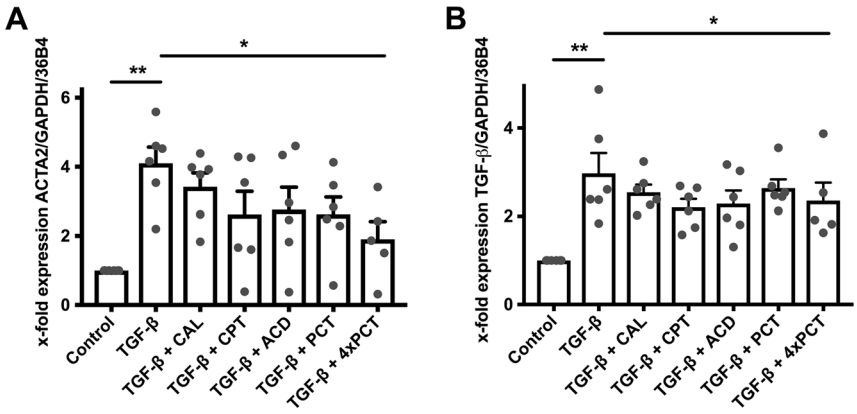

Fig. 5 Effects of calcitriol and vitamin D analogs on mRNA expression in LX-2 cells. **a**, **b** The mRNA expression of ACTA2 and transforming growth factor-β (TGF-β) under stimulation with TGF-β and calcitriol (CAL) or clinically available vitamin D analogs (calcipotriol, CPT; alfacalcidol, ACD; paricalcitol, PCT) was investigated. The values shown are normalized to the control group ($n = 5$–6; $^{*}p < 0.05$; $^{**}p < 0.01$; ANOVA)

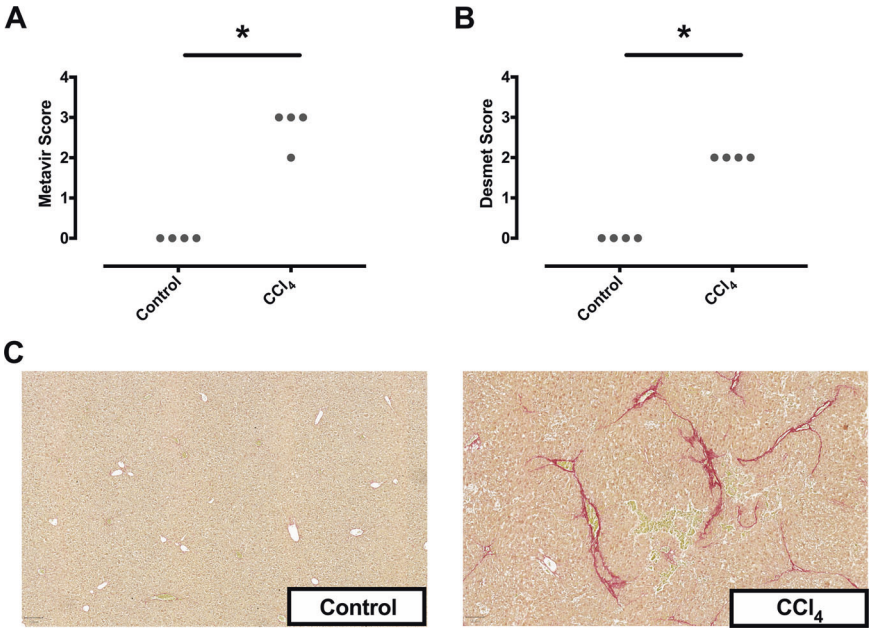

Fig. 6 The CCl_4 protocol used here induces clinically detectible fibrosis after 4 weeks of treatment. Before antifibrotic treatment with vitamin D and its analogs was initiated, the extent of hepatic fibrosis was evaluated in a clinically feasible fashion using histological scoring after 4 weeks of CCl_4 administration. **a**, **b** The clinical histological scoring systems Metavir and Desmet were used for evaluation by pathologists ($n = 4$; $^{*}p < 0.05$; chi-squared test). **c** Representative images of Sirius red staining are shown

hypertension by CAL and propranolol. Interestingly, the authors of that study identified a reduction in intrahepatic resistance (IHR) as one mechanism of action, in addition to a reduction in fibrosis [27]. Among several other mechanisms causing a reduction in IHR, a reduction in angiotensin II-induced HSC contractility by CAL was identified [27].

Another interesting observation was that ACD affected profibrotic stellate cell behavior in vitro. ACD is a prodrug that needs to be activated by hydroxylation at the 25 position [28]. Our finding that ACD exhibited effects in cell culture indicates that murine HSCs, as well as human LX-2 cells, might express relevant enzymes with 25α-hydroxylase activity, as such enzymes are required for the activation of this prodrug.

DXC as another clinically available VD analog also demonstrated antifibrotic efficacy in mHSCs. Owing to its clinical availability we see DXC as an attractive VD analog of high translational value.

We emphasize that our study design reflects a realistic clinical scenario (Fig. 1) in which a therapeutic intervention, performed here with CAL and PCT, is initiated after the induction of detectable liver fibrosis (Fig. 6).

In this respect, our study design differs significantly from that of a former study in which CAL effectively inhibited the development of liver fibrosis in a purely preventive setting [17]. However, in a follow-up study in a therapeutic setting, CAL failed to show remedial effects on established fibrosis [29]. In contrast, Ding et al. [11] showed that CPT ameliorated fibrosis when started 20 days after the induction of liver fibrosis with CCl_4, indicating the therapeutic potency of CPT.

In this study, we clinically evaluated the stage of fibrosis by histological scoring at the beginning of the therapeutic intervention. This aspect is important in regard to clinical translation, as we can more appropriately justify the use of

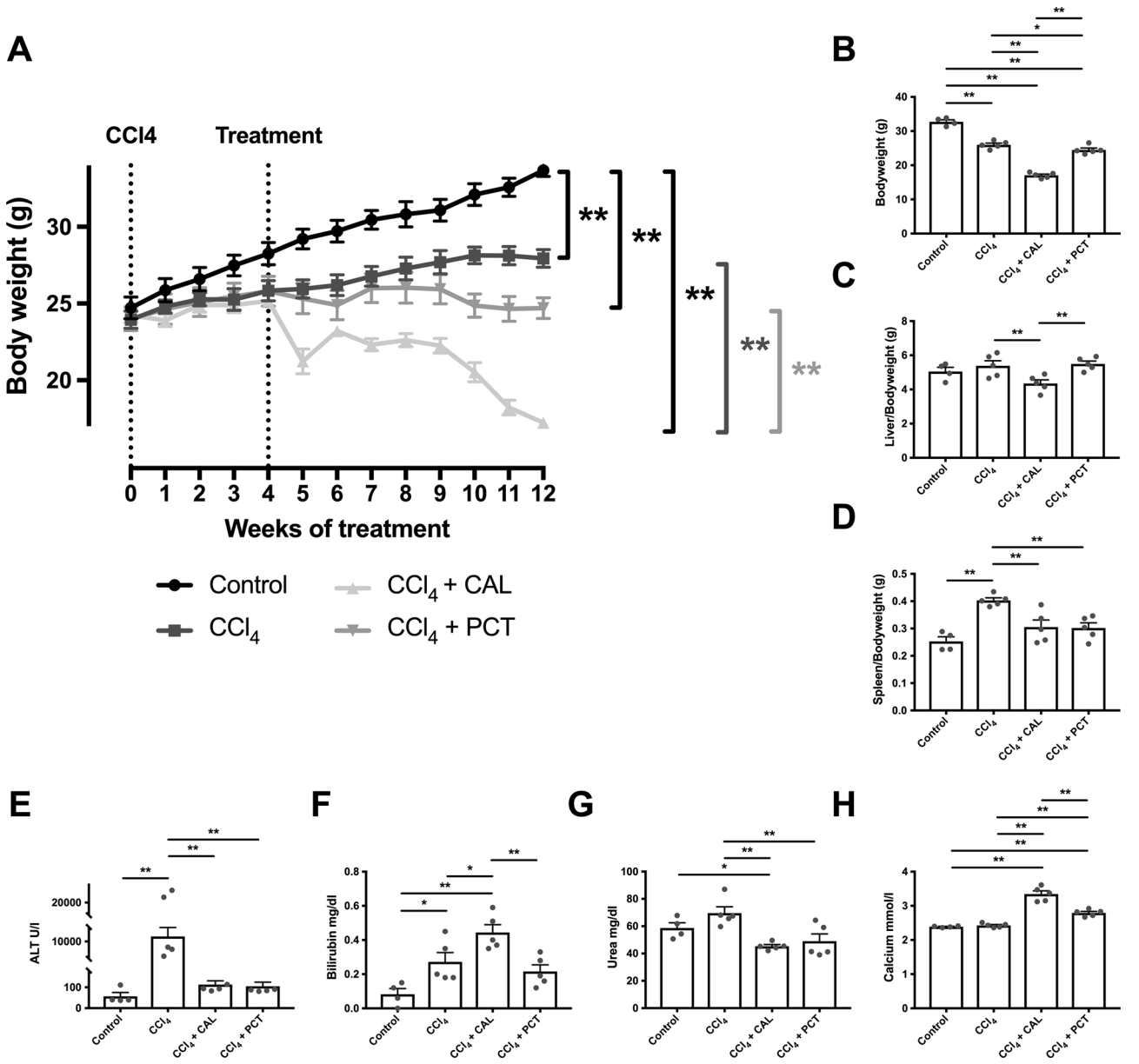

Fig. 7 Effects of calcitriol and paricalcitol on weight and serum parameters in the CCl_4 model. The effects on liver damage and the side effect profile of calcitriol (CAL) and equipotent paricalcitol (PCT) were studied in the CCl_4– model. **a** Body weight was measured over the course of treatment ($n = 4$–5; $^{**}p < 0.01$; ANOVA). **b**–**d** At the end of the experiment, the body weight was measured, and the liver/body weight and spleen/body weight ratios were calculated ($n = 4$–5; $^{*}p < 0.05$; $^{**}p < 0.01$; ANOVA). **e**–**h** Serum parameters were measured under treatment conditions ($n = 4$–5; $^{*}p < 0.05$; $^{**}p < 0.01$; ANOVA)

antifibrotic therapies when we detect fibrosis in a clinically feasible way.

CPT, as a hypocalcemic VD analog, ameliorated liver fibrosis in vivo. Unfortunately, CPT is approved only for clinical use as a topical therapy in patients suffering from psoriasis, but not for systemic use or for other diseases. This limited approval profile is the main reason that we used the hypocalcemic VD analog PCT, which is approved for systemic use to treat secondary hyperparathyroidism, in this study [19]. This decision is relevant; if PCT proves to be effective in humans, off-label use would be possible.

Interestingly, in our study, treatment with both CAL and PCT led to a reduction in inflammatory liver damage, as indicated by the reduction in the ALT level (Fig. 7e) and the significantly lower count of CD11b-positive cells in the liver (Fig. 8c–e). This effect of VD is consistent with our previous findings indicating a reduction in the ALT level and CD11b count under CAL treatment in a model of biliary fibrosis [16].

Despite these anti-inflammatory effects in vivo, no effects of VD or its analogs on the expression of fibrosis- and inflammation-related genes in mKCs, as liver-specific

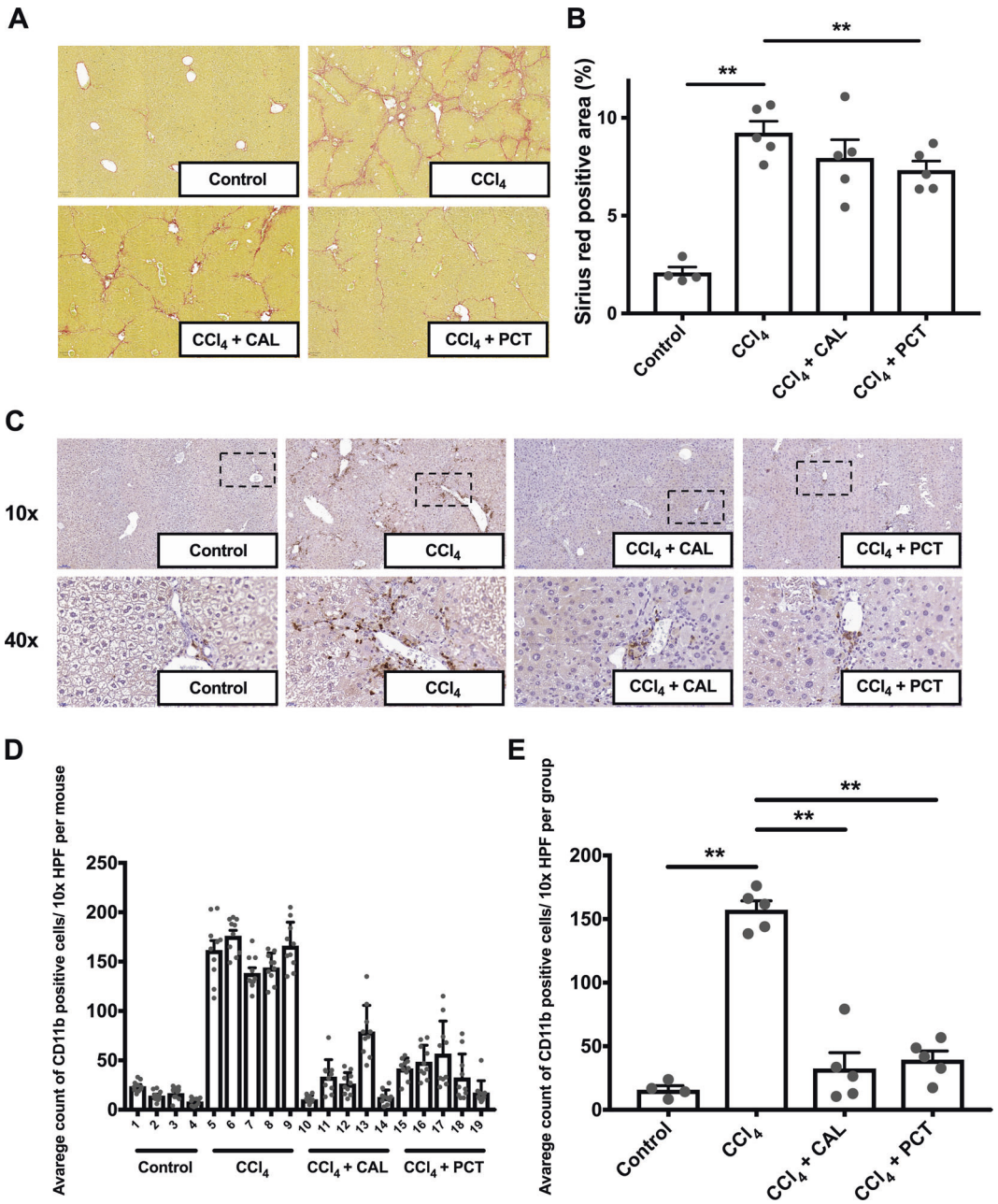

Fig. 8 Calcitriol and paricalcitol inhibit hepatic infiltration by CD11b-positive cells, while the progression of established fibrosis in the CCl_4-model was prevented only by paricalcitol. **a**, **b** The extent of the fibrotic area in Sirius red-stained slides was analyzed using an image analysis system. Representative images and the quantification data for the fibrotic area are shown ($n = 4$–5; $^*p < 0.05$; $^{**}p < 0.01$; ANOVA). **c**–**e** Immunohistochemistry was performed to evaluate the CD11b-positive cell counts in the liver ($n = 4$–5; $^{**}p < 0.01$; ANOVA)

macrophages (Supplementary Fig. 4B-G) expressing functionally active VDR, were detected [10].

Since liver fibrosis is generally asymptomatic and can reflect a long-lasting condition until liver cirrhosis develops, the consideration of the side effect profile of a potentially antifibrotic agent is important. Hypercalcemia is a worrisome side effect of CAL treatment, potentially leading to lethal complications. We hope that hypocalcemic VD analogs have a substantial advantage in this regard. Notably, we demonstrated that PCT-treated animals showed significantly lower calcium levels than CAL-treated animals. In addition, compared to CAL-treated animals, PCT-treated animals did not exhibit such profound weight loss and such distinct hyperbilirubinemia, indicating the more favorable side effect profile of PCT.

The cause of the pronounced weight loss in the CAL group remains unclear. One potential explanation could be that CAL-induced hypercalcemia resulted in adynamia in animals with reduced food intake.

In summary, we described the antifibrotic effects of various VD analogs in vitro. We identified the

hypocalcemic VD analog PCT as superior to CAL in regard to its side effect profile. Furthermore, PCT but not CAL inhibited the progression of fibrosis in the CCl_4 model, emphasizing the potential use of hypocalcemic VD analogs as a promising treatment strategy for chronic liver diseases.

Acknowledgements This work was supported by grants from the *Friedrich-Baur-Stiftung* and the *Förderprogramm für Forschung und Lehre (FöFoLe)* of the Ludwig-Maximilians University Munich. We thank Sebastian Reiter for his support in the illustration of the figures.

Compliance with ethical standards

Conflict of interest Michael Trauner and Gerald Denk would like to make the following disclosures: Michael Trauner received a research grant from Intercept, Albireo, Falk, MSD, Takeda, and Gilead; in addition, he holds a patent for the medical use of Nor-UDCA. Gerald Denk received advisory board and lecture fees and travel support from AbbVie, Falk, Gilead, GMP Orphan, Intercept and Novartis. The other authors declare that they have no conflict of interest.

References

1. Schuppan D, Afdhal NH. Liver cirrhosis. Lancet. 2008;371:838–51.
2. Bosch FX, Ribes J, Diaz M, Cléries R. Primary liver cancer: worldwide incidence and trends. Gastroenterology. 2004;127 (5Suppl 1):S5–16.
3. Caraceni P, Riggio O, Angeli P, Alessandria C, Neri S, Foschi FG, et al. Long-term albumin administration in decompensated cirrhosis (ANSWER): an open-label randomised trial. Lancet. 2018;391:2417–29.
4. Trotter J, Pieramici E, Everson GT. Chronic albumin infusions to achieve diuresis in patients with ascites who are not candidates for transjugular intrahepatic portosystemic shunt (TIPS). Dig Dis Sci. 2005;50:1356–60.
5. Schindler C, Ramadori G. Albumin substitution improves urinary sodium excretion and diuresis in patients with liver cirrhosis and refractory ascites. J Hepatol. 1999;31:1132.
6. Bajaj JS, Tandon P, O'Leary JG, Biggins SW, Wong F, Kamath PS, et al. The impact of albumin use on resolution of hyponatremia in hospitalized patients with cirrhosis. Am J Gastroenterol. 2018;113:1339.
7. Bataller R, Brenner DA. Liver fibrosis. J Clin Invest. 2005; 115:209–18.
8. Ramadori G, Saile B. Portal tract fibrogenesis in the liver. Lab Invest. 2004;84:153–9.
9. Ramadori G, Saile B. Inflammation, damage repair, immune cells, and liver fibrosis: specific or nonspecific, this is the question. Gastroenterology. 2004;127:997–1000.
10. Gascon-Barre M, Demers C, Mirshahi A, Néron S, Zalzal S, Nanci A. The normal liver harbors the vitamin D nuclear receptor in nonparenchymal and biliary epithelial cells. Hepatology. 2003;37:1034–42.
11. Ding N, Yu RT, Subramaniam N, Sherman MH, Wilson C, Rao R, et al. A vitamin D receptor/SMAD genomic circuit gates hepatic fibrotic response. Cell. 2013;153:601–13.
12. Arteh J, Narra S, Nair S. Prevalence of vitamin D deficiency in chronic liver disease. Dig Dis Sci. 2010;55:2624–8.
13. Zhu L, Kong M, Han YP, Bai L, Zhang X, Chen Y, et al. Spontaneous liver fibrosis induced by long term dietary vitamin D deficiency in adult mice is related to chronic inflammation and enhanced apoptosis. Can J Physiol Pharmacol. 2015;93: 385–94.
14. Paternostro R, Wagner D, Reiberger T, Mandorfer M, Schwarzer R, Ferlitsch M, et al. Low 25-OH-vitamin D levels reflect hepatic dysfunction and are associated with mortality in patients with liver cirrhosis. Wien Klin Wochenschr. 2017;129:8–15.
15. Amanzada A, Goralczyk AD, Moriconi F, van Thiel DH, Ramadori G, Mihm S. Vitamin D status and serum ferritin concentration in chronic hepatitis C virus type 1 infection. J Med Virol. 2013;85:1534–41.
16. Reiter FP, Hohenester S, Nagel JM, Wimmer R, Artmann R, Wottke L, et al. 1,25-(OH)(2)-vitamin D(3) prevents activation of hepatic stellate cells in vitro and ameliorates inflammatory liver damage but not fibrosis in the Abcb4(-/-) model. Biochem Biophys Res Commun. 2015;459:227–33.
17. Abramovitch S, Dahan-Bachar L, Sharvit E, Weisman Y, Ben Tov A, Brazowski E, et al. Vitamin D inhibits proliferation and profibrotic marker expression in hepatic stellate cells and decreases thioacetamide-induced liver fibrosis in rats. Gut. 2011;60: 1728–37.
18. Bjelakovic G, Nikolova D, Bjelakovic M, Gluud C. Vitamin D supplementation for chronic liver diseases in adults. Cochrane Database Syst Rev. 2017;11:CD011564.
19. Sprague SM, Llach F, Amdahl M, Taccetta C, Batlle D. Paricalcitol versus calcitriol in the treatment of secondary hyperparathyroidism. Kidney Int. 2003;63:1483–90.
20. Reiter FP, Wimmer R, Wottke L, Artmann R, Nagel JM, Carranza MO, et al. Role of interleukin-1 and its antagonism of hepatic stellate cell proliferation and liver fibrosis in the Abcb4(-/-) mouse model. World J Hepatol. 2016;8:401–10.
21. Liu C, Tao Q, Sun M, Wu JZ, Yang W, Jian P, et al. Kupffer cells are associated with apoptosis, inflammation and fibrotic effects in hepatic fibrosis in rats. Lab Invest. 2010;90:1805–16.
22. Bell E, Ivarsson B, Merrill C. Production of a tissue-like structure by contraction of collagen lattices by human fibroblasts of different proliferative potential in vitro. Proc Natl Acad Sci USA. 1979;76:1274–8.
23. Intraobserver and interobserver variations in liver biopsy interpretation in patients with chronic hepatitis C. The French METAVIR Cooperative Study Group. Hepatology. 1994;20(1 Pt 1):15–20.
24. Desmet VJ, Gerber M, Hoofnagle JH, Manns M, Scheuer PJ. Classification of chronic hepatitis: diagnosis, grading and staging. Hepatology. 1994;19:1513–20.
25. Kolios G, Valatas V, Kouroumalis E. Role of Kupffer cells in the pathogenesis of liver disease. World J Gastroenterol. 2006;12: 7413–20.
26. Zhang X, Yu WP, Gao L, Wei KB, Ju JL, Xu JZ. Effects of lipopolysaccharides stimulated Kupffer cells on activation of rat hepatic stellate cells. World J Gastroenterol. 2004;10: 610–3.
27. Lee PC, Yang YY, Lee WP, Lee KC, Hsieh YC, Lee TY, et al. Comparative portal hypotensive effects as propranolol of vitamin D(3) treatment by decreasing intrahepatic resistance in cirrhotic rats. J Gastroenterol Hepatol. 2015;30:628–37.
28. Kubodera N. A new look at the most successful prodrugs for active vitamin D (D hormone): alfacalcidol and doxercalciferol. Molecules. 2009;14:3869–80.
29. Abramovitch S, Sharvit E, Weisman Y, Bentov A, Brazowski E, Cohen G, et al. Vitamin D inhibits development of liver fibrosis in an animal model but cannot ameliorate established cirrhosis. Am J Physiol Gastrointest Liver Physiol. 2015;308:G112–120.